A compartmentalized microsystem helps understanding the uptake of benzo[a]pyrene by fungi during soil bioremediation processes

Claire Baranger, Isabelle Pezron, Laurence Lins, Magali Deleu, Anne Le Goff, Antoine Fayeulle

▶ **To cite this version:**

Claire Baranger, Isabelle Pezron, Laurence Lins, Magali Deleu, Anne Le Goff, et al.. A compartmentalized microsystem helps understanding the uptake of benzo[a]pyrene by fungi during soil bioremediation processes. Science of the Total Environment, 2021, 784, pp.147151. 10.1016/j.scitotenv.2021.147151 . hal-03201329

HAL Id: hal-03201329
https://utc.hal.science/hal-03201329v1

Submitted on 9 May 2023

HAL is a multi-disciplinary open access archive for the deposit and dissemination of scientific research documents, whether they are published or not. The documents may come from teaching and research institutions in France or abroad, or from public or private research centers.

L'archive ouverte pluridisciplinaire **HAL**, est destinée au dépôt et à la diffusion de documents scientifiques de niveau recherche, publiés ou non, émanant des établissements d'enseignement et de recherche français ou étrangers, des laboratoires publics ou privés.

Distributed under a Creative Commons Attribution - NonCommercial 4.0 International License

Version of Record: https://www.sciencedirect.com/science/article/pii/S004896972102221X
Manuscript_ae507990b8b5e5d220e6ec20563a689f

A compartmentalized microsystem helps understanding the uptake of benzo[a]pyrene by fungi during soil bioremediation processes

Claire Baranger[1], Isabelle Pezron[1], Laurence Lins[2], Magali Deleu[2], Anne Le Goff[3*], Antoine Fayeulle[1*]

[1] Université de technologie de Compiègne, ESCOM, TIMR (Integrated Transformations of Renewable Matter), Centre de Recherche Royallieu - CS 60 319 - 60 203 Compiègne Cedex, France

[2] TERRA Research Center, Laboratory of Molecular Biophysics at Interfaces, SFR Condorcet, Gembloux Agro-Bio Tech, University of Liege, Passage des Déportés, 2, 5030 Gembloux, Belgium

[3] Université de technologie de Compiègne, CNRS, Biomechanics and Bioengineering, Centre de recherche Royallieu - CS 60 319 - 60 203 Compiègne Cedex, France

[*] Corresponding authors: antoine.fayeulle@utc.fr; anne.le-goff@utc.fr

© 2021 published by Elsevier. This manuscript is made available under the CC BY NC user license
https://creativecommons.org/licenses/by-nc/4.0/

Abstract

Hydrophobic organic soil contaminants such as polycyclic aromatic hydrocarbons (PAH) are poorly mobile in the aqueous phase and tend to sorb to the soil matrix, resulting in low bioavailability. Some filamentous fungi are efficient in degrading this kind of pollutants. However, the mechanism of mobilization of hydrophobic compounds by non-motile microorganisms such as filamentous fungi needs investigations to improve pollutant bioavailability and bioremediation efficiency. Usual homogeneous media for microbial growth in the lab are poorly suited to model the soil, which is a compartmentalized and heterogeneous habitat.

A microfluidic device was designed to implement a compartmentalization of the fungal inoculum and the source of the pollutant benzo[a]pyrene (BaP) as a deposit of solid crystals in order to gain a further insight into the mechanisms involved in the access to the contaminant and its uptake in soils. Thus in this device, two chambers are connected by an array of parallel microchannels that are wide enough to allow individual hyphae to grow through them. Macro-cultures of *Talaromyces helicus* in direct contact with BaP have shown its uptake and intracellular storage in lipid bodies despite the low propensity of BaP to cross aqueous phases as shown by simulation. Observations of *T. helicus* in the microfluidic device through laser scanning confocal microscopy indicate preferential uptake of BaP at a close range and through contact with the cell wall. However faint staining of some hyphae before contact with the deposit also suggests an extracellular transport phenomenon. Macro-culture filtrates analyses have shown that *T. helicus* releases extracellular non-lipidic surface-active compounds able to lower the surface tension of culture filtrates to 49.4 mN/m. Thus, these results highlight the significance of active mechanisms to reach hydrophobic contaminants before their uptake by filamentous fungi in compartmentalized micro-environments and the potential to improve them through biostimulation approaches for soil mycoremediation.

Key words

Bioavailability; Biodegradation; Biosurfactant; Microfluidic device; Mycoremediation; Polycyclic aromatic hydrocarbons

1 Introduction

Soil is a complex environmental compartment resulting from the weathering of parental rock under the combined action of living organisms, surface water and the atmosphere. As a support for human activities, soil is heavily affected by pollution and notably with persistent pollutants, which is a major source of soil quality alteration (Panagos *et al.*, 2013). Among these pollutants, some families of organic contaminants including polycyclic aromatic hydrocarbons (PAH), polychlorobiphenyls, and various xenobiotics and pesticides, are highly hydrophobic and persistent in soils. Due to their carcinogenicity and high persistence in the environment, PAH are among the most regulated pollutants in environmental policies (Jennings, 2012). Such poorly water-soluble contaminants can be present in non-aqueous-phase liquids, tar or solid particles. Moreover, they tend to strongly sorb to soil aggregates and organic matter (Ortega-Calvo *et al.*, 2013). These properties make them poorly available for degradation by microorganisms (Posada-Baquero *et al.*, 2019).

Bioremediation corresponds to the use of biological activities in particular of microorganisms to destroy pollutants or decrease the associated risks for humans and the environment. It is regarded as a low-technology and low-cost approach with a higher degree of public acceptance in comparison to other physicochemical remediation techniques more destructive of the living fraction and the structure of soils such as high temperature incineration, chemical decomposition, solvent extraction or UV oxidation (Vidali, 2001). Thus bioremediation is one of the established methods undergoing the highest development for PAH cleanup in soils (Kuppusamy et al., 2017). One of the parameters that can impair bioremediation efficiency is the low competitiveness and adaptability of microbial inocula (Rayu et al., 2012), which could be prevented by the use of telluric strains. Soil is a divided environment consisting in solid, aqueous and gas phases, hosting a great variety of living organisms, including fungi. Among microorganisms, micromycetes are particular in the sense that they do not need water as a support for dispersal, and can form aerial structures. This allows mycelium to occupy vast volumes of soil and come into contact with several phases. Indeed, soil fungi are known for their ability to form mycelial networks in three dimensions that constitute large exchange surfaces within

the soil porosities, and to mobilize nutritious substrates through the release of extracellular lytic enzymes before substrates incorporation (Moore *et al.*, 2015). Notably, micromycetes play important roles in hydrophobic organic pollutants dynamics within the soil matrices (Baranger *et al.*, 2021).

Hydrocarbons can be a source of carbon and energy for fungi. In non-ligninolytic fungi, the main metabolic pathway described as involved in PAH biodegradation is the cytochrome P450 pathway. Cytochrome P450 mono-oxygenases are a family of intracellular enzymes involved in the oxidation of various hydrophobic substrates (Črešnar and Petrič, 2011). Cytochrome P450 monooxygenases initiate the oxidation of PAH into arene oxides that are further metabolized into phenol and dihydrodiol derivatives (Cerniglia and Sutherland, 2010). This intracellular degradation pathway implies preliminary uptake of hydrocarbons and notably PAH by fungal cells.

Lindley and Heydemann (1986) first described the incorporation of dodecanol into whole cells of *Cladosporium resinae* by early adsorption to the cell surface followed by active uptake. More recent studies have focused on the uptake of various hydrophobic organic pollutants including polycyclic aromatic hydrocarbons (PAH). PAH have been described to behave in a similar way to neutral lipids, diffusing into lipid membranes (Castelli *et al.*, 2002) and being incorporated in lipid storage sites in fungal cells (Verdin *et al.*, 2005; Chang *et al.*, 2015). Notably, the ubiquitous PAH benzo[a]pyrene (BaP) can be localized in lipid bodies in mycelium that has been cultivated in contact with this pollutant (Verdin *et al.*, 2005; Fayeulle *et al.* 2014). However, an active transport mechanism for BaP uptake dependent on the fungal cytoskeleton has been highlighted in *Fusarium solani,* and active phenomena may be involved in BaP mobilization before its uptake by the same fungus (Fayeulle *et al.*, 2014). Interestingly, an active secondary transport mechanism was recently proposed for the uptake of monoaromatic compounds by *Phanerochaete chrysosporium* (Leriche-Grandchamp *et al.*, 2020).

Some micro-organisms are able to release biosurfactants, which can partially solubilize hydrophobic substrates and have been studied for the dispersal of hydrocarbons. In fungi, biosurfactants and emulsifiers are involved in nutrition for the mobilization of fats and adhesion to hydrophobic surfaces (Käppeli *et al.*, 1984). Modulations of cell surface hydrophobicity drive the attachment to surfaces

and utilization of hydrophobic substrates (plant leaf wax, oils…) and can affect the fungal interaction with hydrophobic pollutants (Puchkov *et al.*, 2002; Arutchelvi *et al.*, 2008; Garay *et al.*, 2018). Adsorption of hydrophobic substrates on the cell surface is thus thought to be a determining step prior to potential uptake by the cells (Fayeulle, 2013; Al-Hawash *et al.*, 2019). It is known that surfactants are released in the aqueous phase and accumulate at solid/water and air/water interfaces. However the interaction of fungal surfactants with hydrophobic soil contaminants and their potential contribution to pollutant mobilization is poorly understood.

Talaromyces helicus is a filamentous soil ascomycete with a cosmopolitan distribution, found on several continents in temperate to tropical climates (Huang and Schmitt, 1975; Romero *et al.*, 2009; Scervino *et al.*, 2010; Olagoke, 2014; Wu *et al.*, 2016; Fayeulle *et al.*, 2019). It can grow at moderate temperatures (20°C) and presents relatively fine hyphae of 1 to 3 µm in diameter (Baranger *et al.*, 2020) able to penetrate microporosities and narrow cracks in the substrate, thus potentially covering large volumes of soil. This species has been isolated from contaminated soils, showing the resistance of some strains to pollutions, and its adaptation to the soil environment (Fayeulle *et al.*, 2019). Thus, *T. helicus* has been identified as holding potential for the bioremediation of multiple contaminations due to the bioaccumulation of heavy metals and the biodegradation of several organic pollutants including isoproturon, biphenyl and benzo[a]pyrene (Romero *et al.*, 2005, 2009, 2010; Fayeulle *et al.*, 2019). The particular efficiency of *T. helicus* to improve PAH biodegradation in industrial soils with aged mixed contaminations was also highlighted at the microcosm scale (Fayeulle *et al.*, 2019).

In this study, we aim to investigate the biodegradation of BaP *by T. helicus* at the microscopic scale, which corresponds both to the size of fungal hyphae and to that of soil aggregates, and is therefore a natural scale to study soil microbial processes (Wilpiskeski *et al.,* 2019). Microfluidics offer the possibility to design model microenvironments with a good control of their geometry and chemical properties, taking advantage of the specific properties of small scale fluid flows to finely tune mechanical forces and mass transfers (Squires and Quake, 2005). Transparent microfluidic devices, usually made of glass or silicon rubber, can be used as soil models (Aleklett *et al.*, 2018) and

accommodate the growth of plant roots (Grossmann *et al.*, 2011), bacterial communities (Alnahhas *et al.*, 2019) or fungi (Held *et al.*, 2010). Parameters such as hyphal growth velocity can be measured by videomicroscopy and can be used to assess the ability of a fungal strain to colonize a polluted porous matrix (Baranger *et al.*, 2020).

In this work, we used a microfluidic device in which the model pollutant and the fungus were introduced in two separate compartments. The aim of such an experiment is to elucidate whether a filamentous fungus needs to grow in contact to the pollutant source for its uptake and degradation, or whether prior extracellular mobilization mechanisms are required to enhance the pollutant bioavailability in the aqueous phase. The investigation of this biological process is important for future optimizations of PAH mycoremediation protocols in soils through biostimulation approaches. This study is the first one to our knowledge to use a microfluidic device in order to study pollutants mobilization mechanisms by microorganisms in soil.

2 Materials and methods

2.1 Fungal strain

A strain of the filamentous fungus *Talaromyces helicus* from our laboratory collection and previously isolated from an industrial contaminated soil from North of France was used for this study. Identification of the strain occurred through molecular approach by BCCM™/MUCL (Louvain-la-Neuve, Belgium) based on sequencing ITS region, elongation factor gene, or β-tubulin gene, in complement of the macro- and micro-morphological features of pure cultures. The strain was maintained on MYEA solid medium (malt extract 20 g/L – Condalab, Madrid, Spain; yeast extract 2 g/L – VWR, Fontenay-sous-Bois, France; microbiological grade agar 15 g/L – Becton Dickinson, Rungis, France), at 22°C with a 12 h - 12 h light-dark cycle, and transplanted onto fresh medium every ten days.

Fresh mycelium was produced in a rich medium (MYPC) containing malt extract 10 g/L, yeast extract 4 g/L, soy peptone 10 g/L (Merck, Darmstadt, Germany) and casamino-acids 2 g/L. Shaking flasks

containing 50 mL MYPC were inoculated with spores of *T. helicus* to reach a final concentration of 10^4 spores/mL.

2.2 Off-ship incubation with benzo[a]pyrene and lipid staining

T. helicus cultures with BaP were prepared in mineral medium supplemented with glucose (MMG) at pH 5.5, as described by (Fayeulle *et al.*, 2019). MMG is comprised of KCl 0.25 g/L, $NaH_2PO_4.2H_2O$ 1.54 g/L, Na_2HPO_4 8 mg/L, $MgSO_4.7H_2O$ 0.25 g/L, NH_4NO_3 1 g/L, $ZnSO_4.7H_2O$ 1 mg/L, $MnCl_2.H_2O$ 0.1 mg/L, $FeSO_4.7H_2O$ 1 mg/, $CuSO_4.5H_2O$ 0.5 mg/L, $CaCl_2.2H_2O$ 0.1 mg/L, MoO_3 0.2 mg/L and glucose 20 g/L. Mineral salts and glucose were purchased from Thermo Fisher Scientific (Illkirch-Graffenstaden, France). Prior to adding the medium, 50 µg of BaP (Sigma Aldrich, Haverhill, United Kingdom) was introduced in each flask by pipetting the correct amount of a BaP stock solution in acetone (0.8 g/L), and allowing the acetone to evaporate under a fume hood. Shaking flasks were inoculated with fresh mycelium of *T. helicus* that was pre-grown in MYPC, and were then incubated for 24h. After incubation, mycelium pellets were mounted on a microscope slide and observed in bright field and epifluorescence microscopy or in laser scanning confocal microscopy.

Lipids were stained *in vivo* on fresh mycelium samples taken from liquid cultures, using BODIPY 500/510 lipid dye (Thermo Fischer Scientific – Illkirch-Graffenstaden, France). The stock solution of BODIPY in DMSO was pipetted directly onto mycelium samples mounted on a glass microscope slide, achieving a final dye concentration of 0.1 µM/mL.

2.3 Production and detection of surface-active compounds

Shaking flasks containing MMG were inoculated with spores of *T. helicus* to reach a final concentration of 10^4 spores/mL. 50 mL flasks containing 10 mL medium were used for the growth kinetics experiment, and 250 mL flasks containing 50 mL medium were used for filtrates production before characterization. Cultures were incubated at 22°C with orbital shaking and a 12 h/12 h light-dark cycle. The mycelium was harvested by vacuum-filtration on quantitative filter paper (VWR 434) with a Büchner funnel. Filtrates were collected, filtered again on a 0.2 µm syringe filter to sterilize

154 them and remove any remaining particle, and frozen at -20°C until use. To quantify fungal growth in
155 10 mL cultures, the paper filters with mycelium cake were rinsed with distilled water and dried in a
156 105°C oven for 24 h, then weighted. For the growth kinetics experiments, 10 mL cultures were done
157 in triplicate and filtered separately.
158 Surface tension in filtrates was measured on a tensiometer (Krüss K-100) with the Wilhelmy plate
159 method. Each measurement was taken 10 minutes after immersing the plate into the sample, to
160 allow the meniscus to equilibrate at room temperature. All measurements were performed on
161 triplicate samples, and results are presented as average values and standard deviations for each
162 triplicate.

163 **2.4 High-Performance Thin-Layer Chromatography**

164 High-Performance Thin-Layer Chromatography (HPTLC) analysis of culture filtrates was conducted by
165 the CAP DELTA laboratory at Chromacim (Grabels, France) with the CAMAG method. Soy lecithin (1
166 g/L), bovine serum albumin (1 g/L) and glucose (1 g/L) were used as positive controls for the
167 detection of lipids, proteins and reducing sugars respectively. 10 µL of each control was deposited on
168 the plate, as well as 50 µL of the crude filtrate. Samples were deposited on a TLC plate coated with
169 F254 silica gel with an application spray ATS 4 and migrated vertically in a saturated ADC2 chamber
170 over 20 min (migration distance of 70 mm). The mobile phase was a cosolvent mixture containing
171 $CHCl_3$:CH_3OH:H_2O:NH_3 32 % (32:15:2:1 in volume).
172 After migration, thin layer plates were imaged under white light, UV 254 nm, UV 366 nm and scanned
173 at 200 nm. Then a revelation was done with a primulin reagent (0.1 g/L in acetone:water 80:20 by
174 volume) before imaging under white light, UV 366 nm and scanning at 366 nm for the detection of
175 aliphatic carbon chains corresponding to lipids. Finally a revelation with an anisaldehyde reagent (4-
176 methoxybenzaldehyde at 0.5% v/v in CH_3OH:CH_3COOH:H_2SO_4 42.5:5:2.5 by volume) was carried out
177 as well as imaging under white light and UV 366 nm for the detection of ketone, aldehyde and alcohol
178 functions corresponding mostly to carbohydrates.

2.5 Microfabrication

Microfluidic chips for fungal culture were fabricated by soft lithography as described by Baranger *et al.* (2020). The pattern was imprinted on a silicon wafer using two layers of SU8 photoresist (Microfactory, IPGG, Paris): a first layer comprised of the microchannel pattern with an average thickness of 5.8 ± 0.3 µm, and a second layer forming the culture chambers, with an average thickness of 124 ± 2 µm. Polydimethylsiloxane (PDMS, Sylgard 184, Dow Corning) mixed with 10% reticulating agent was cast against the wafer and allowed to cure for at least 2 h at 70°C. Inlets were added by punching holes through the PDMS with a biopsy puncher (2 mm for the inoculation well, 1 mm for medium injection inlets). The negatively patterned PDMS slab was bound to a clean glass microscope slide or cover slip after surface oxidization in an oxygen plasma chamber (Harrick) for 60 s.

2.6 On-chip fungal culture

All chips were filled with sterile MMG prior to seeding with mycelium. A 2 mm diameter mycelium plug was collected from a solid-medium culture of *T. helicus* at the edge of the growing colony, and transferred to the inoculation inlet of the chip. The inlet was then closed with a PDMS plug to prevent drying. 1 µL of BaP stock solution (0.8 g/L in acetone) was pipetted into one of the injection inlets on the opposite side to the inoculation chamber right after inoculation. Upon contact with the aqueous culture medium, BaP immediately precipitated into crystals localized at the injection inlet. The microchips were then placed in a sealed Petri dish in a water-saturated atmosphere. The mycelium was allowed to grow at 22°C with a 12 h - 12 h light-dark cycle in static conditions. Mycelial growth in the device and fluorescent staining of the cells due to BaP uptake were monitored in the chips for up to 8 days.

2.7 Microscopy imaging and image processing

Mycelia of *T. helicus* grown in liquid cultures with BaP and mounted between slide and coverslip were imaged in bright field and epifluorescence using an OLYMPUS BX60 microscope mounted with a color

Infinity 3-6UR camera (Lumenera). Time-lapse epifluorescence microscopy observations were performed using a DMI-8 inverted microscope (Leica) equipped with a motorized stage and a DFC 3000G camera (Leica). The fluorescence of BaP was observed with a standard DAPI emission filter set. Microchips inoculated with *T. helicus* and spiked with BaP were imaged using a confocal laser scanning microscope (LSM 710 Axio Observer, Carl Zeiss). The fluorescent signal of BaP was detected using the DAPI filter (excitation 405 nm, emission 453 nm) and that of BODIPY using the FITC filter (excitation 488 nm, emission 563 nm).

All image processing and measurements were carried out using ImageJ. For the BODIPY co-staining experiment, mycelium mounted on a glass slide was imaged in confocal microscopy at 40x magnification with z increments of 0.38 µm, and maximum intensity projections along z were made. For the on-chip fungal culture experiments, stacks of 11 images with a 1 µm increment were projected along z. Average grey intensity was measured over rectangular areas of 10x100 µm (12x121 pixels) in 3 separate microchannels on each image. Results are presented as mean and standard deviation of the 3 measurements for each time point.

2.8 In silico simulation

The penetration of BaP through a model lipid bilayer was simulated using the IMPALA method as first described by Ducarme *et al.* (1998). Briefly, this method is based on a Monte Carlo approach using an implicit description of membrane. The latter is described as a continuous medium whose properties vary along the axis perpendicular to the bilayer plane (z axis). The force field was parameterized to mimic a membrane in aqueous environment by considering (1) the hydrophobic effect between the membrane and a solute (Epho) and (2) the perturbation effect of the solute on the lipid acyl chain organization (Elip). The two restraints were calculated and summed at each position of BaP into the implicit membrane and the molecule was systematically moved along the z axis by 1 A steps, from one side of the membrane to the other. The method yields a profile of the interaction energy for each position along the Z axis, the most stable positions being those with minimal energy.

3 Results

3.1. Benzo[a]pyrene diffusion in lipid phases

BaP is highly hydrophobic (log K_{ow} = 6.35) and has an extremely low solubility in water ($3.8 \cdot 10^{-3}$ mg/L at 25°C) (IARC, 2012). This compound forms solid crystals when added to aqueous media such as those used for microbial cultures. In soil, it is associated to solid particles and organic matter, but can also be present in hydrocarbon mixtures as non-aqueous phase liquids (Ortega-Calvo *et al.*, 2013).

The intracellular uptake of BaP in fungal cells implies that the molecule reaches cell surfaces and transport occurs through the plasma membrane. In order to predict the interaction of BaP with biological membranes, its penetration into an implicit symmetrical lipid bilayer was simulated by the IMPALA method (Fig. 2 a). As expected for a hydrophobic molecule, the profile displayed a sharp contrast between the positions corresponding to the water phase surrounding the membrane and those corresponding to the hydrocarbon core of the membrane. The most stable positions for BaP, displaying negative interaction energies, are located between -14 Å and 14 Å, and correspond to the alkyl core of the model lipid bilayer. In contrast, the interaction energy is maximal above -22 Å and 22 Å, and decreases sharply between (-)22 Å and (-)14 Å. This decrease coincides with positions where the BaP molecule is in contact with the membrane, and still partially surrounded by water. Indeed, for a 36 Å thick membrane, the hydrated phosphate heads of the amphiphilic lipids are located between 14 and 18 Å.

The energy profile obtained predicts that the BaP molecule is most stable at the core of lipid bilayers, This result is consistent with the low solubility in water of BaP, which tends to minimize its contact surface with aqueous phases.

3.2. Intracellular localization of benzo[a]pyrene in *Talaromyces helicus*

Since BaP emits a blue fluorescent signal when excited with UV light, its incorporation into the fungal biomass can be visualized directly through epifluorescence microscopy. Off-chip observations of *T. helicus* mycelium pellets incubated with BaP for 24 h were thus carried out. In control flasks without

253 BaP, a slight fluorescence of the mycelium was visible under UV (Fig. 2 b). The fluorescent signal
254 observed without addition of any fluorophore corresponds to the autofluorescence of parietal
255 components. Indeed, fungal hyphae are known to emit blue autofluorescence when exposed to UV
256 light (330-385 nm) due to the presence of chitin in the fungal wall (Jabaji-Hare *et al.*, 1984; Dreyer *et*
257 *al.*, 2006).
258 After 24 h of incubation with BaP, the mycelium pellets appeared brightly fluorescent at their core,
259 which could be due to the immediate contact with BaP crystals trapped in the hyphal network. Blue
260 fluorescence was detected along hyphae, with cell walls and septa appearing more strongly stained
261 than the cytoplasm. Many intracellular vesicles were visible in bright field, and appeared brightly
262 fluorescent. In some hyphal tips, these vesicles were distributed in the cytoplasm. In mature hyphae,
263 the vesicles were localized at the periphery of the cytoplasm, while vacuoles were not stained (Fig. 2
264 b). When mycelium previously incubated with BaP was stained with BODIPY and observed in confocal
265 microscopy, blue and green fluorescent signals co-localized in lipid bodies indicating BaP intracellular
266 storage in these organelles (Fig. 2 c).

267 **3.3. Detection of fungal surface-active molecules**

268 Culture filtrates of *T. helicus* were harvested and analyzed through surface tension measurements to
269 detect potential fungal surfactants (Fig. 3 a). Surface tension in culture filtrates decreased over time
270 and reached a minimum after 6 days, stabilizing until the end of the experiment (after 13 days). The
271 surface tension was lowered to 49.4 ± 0 mN/m, compared to 69 ± 3.7 mN/m in fresh, sterile mineral
272 medium. This result clearly demonstrates the presence of surface-active compounds in the
273 extracellular medium. Extracellular proteins or biosurfactants secreted by the fungus may be
274 responsible for this decrease.
275 In order to gather more information on the chemical nature of these surfactants, culture filtrates
276 harvested after 13 days of incubation were analyzed in high performance thin-layer chromatography
277 (Fig. 3.b). 13-day filtrates were chosen because they contain the lowest glucose contents, which can

interfere with the results and make it difficult to concentrate the samples. After migration, six main spots were detected through 254nm UV illumination, which reveals organic compounds in a non-specific way. The most intense spot was detected at 0.05 Rf and corresponds to residual glucose in the sample. Five fainter spots were detected at 0.08, 0.16, 0.38, 0.60 and 0.77 Rf. After spraying with a primulin solution to detect lipids and imaging at 266 nm, the only visible spot corresponded to the migration coefficient of glucose. Finally, anisaldehyde revelation was used to reveal carbohydrates. Spots at 0.08, 0.16, 0.60 Rf and the glucose spot reacted with anisaldehyde, but not the spots appearing at 0.60 and 0.77 Rf. In addition, a new spot at 0.72 Rf was visible in white light with anisaldehyde revelation. This compound may be present in concentrations too low for the spot to be visible without prior staining.

The filtrate is a mixture of several compounds with various affinities with the organic phase, which appears to be predominantly made of carbohydrates, and not lipids. Peptides were not investigated in HPTLC, however protein quantification in the filtrates through the Bradford method show the presence of extracellular protein in low amounts with the highest concentration at 3 mg/L after 10 days of incubation.

3.4 Benzo[a]pyrene mobilization in a compartmentalized device

T. helicus was grown in microfluidic chips spiked with BaP, and the mycelium was observed at different growth stages. The mycelium was imaged in bright field to monitor growth and locate the edge of the colony. Chips were then observed in laser scanning confocal microscopy to detect the fluorescent staining of hyphae due to BaP incorporation.

Fig. 4 a shows the evolution of the fluorescent staining over time at two observations points in the same chip: in chamber A close to the inoculum (left column) and in chamber B right at the opening of microchannels (right column). Fig. 4 b represents the position of the different elements within the chip geometry. The intensity of the fluorescent staining increased over time. After 4 days of incubation, the mycelium had grown into the inoculation chamber A but did not yet reach chamber B.

Faint and diffuse staining of the hyphae was observed, but not more intense than the natural autofluorescence of the mycelium observed in control chips without BaP. After 5 days, hyphae reached the channels but not BaP crystals yet and the mycelium fluorescence appears still low. After 6 days and even more after 7 days, staining intensity clearly increased and was not uniform across the mycelium, i.e. single stained hyphae were distinguishable and appeared more brightly fluorescent than others in contrast to the control (Fig. 4 a). No distinct stained vesicles were visible at 20x magnification. Microchannels enabled the quantification of grey intensity over time in the same area (Fig 4 c). The average fluorescence intensity appears to increase between 3 and 5 days, whereas it remains stable in the control over the whole experiment, which evokes a BaP uptake before direct contact between hyphae and BaP crystals occurred. However the difference of grey intensities between test with BaP and control starts to be statistically significant after 7 days when direct contact between the mycelium and the BaP deposit occurs.

In order to better locate the fluorescence within hyphae, several chips were observed at greater magnification (40X) after 6 and 7 days. Growth velocity was greatly variable from one chip to the other, as previously assessed in the same device with this fungal strain (Baranger *et al.*, 2020). As a result, after 7 days of incubation the mycelium had not reached the BaP deposit in all of the chips (Fig. 5 a and b). In some of the chips where direct contact happened, staining of the mycelium was detected in chamber B. Stained apices were observed at the growth front, in close vicinity to the deposit (Fig. 5 c). In these apices, no lipid bodies were distinguishable and the whole cytoplasm appeared fluorescent. This could be due to the presence of numerous, closely packed lipid droplets that could not be resolved with the camera used. Indeed, the resolution of the images was 0.21 µm/pixel at 40x magnification, while some of the lipid droplets detected in stained apices with the Lumenera camera (used for epifluorescence images) could be as small as 0.2 µm. In mature, ramified hyphae located in the chamber, and directly in contact with the crystals, stained vesicles were clearly visible (Fig. 5 d). Some hyphae in the microchannels were stained as well (not shown). The stained

328 structures were similar to those observed in mycelium grown in liquid medium supplemented with
329 BaP, as described in paragraph 3.2.
330 Interestingly, in chips imaged before the mycelium had reached the deposit, fluorescent staining
331 different from mycelia grown without BaP was observed as well. Indeed, faintly stained apices were
332 visible at the growth front of the mycelium growing through the microchannels (Fig. 5 a). Some
333 hyphae localized in chamber B, closer to the BaP deposit, displayed a stronger staining and visible
334 intracellular lipid bodies (Fig. 5 b). The cell wall and some septa appeared to be stained as well. The
335 stained lipid bodies were smaller and less numerous than they were in hyphae in contact with BaP
336 crystals (Fig. 5 d).

337 **4 Discussion**

338 **4.1. Benzo[a]pyrene storage in lipid bodies**

339 Epifluorescence observations with a co-staining with BODIPY confirm that BaP is absorbed into the
340 cells of *T. helicus* and stored in lipid bodies. Similar observations were made in the saprotrophic
341 fungus *Fusarium solani* (Verdin *et al.*, 2005; Fayeulle *et al.*, 2014) as well as other fungal strains
342 including the yeast *Saccharomyces cerevisiae,* the white rot *Phanerochaete chrysosporium* (Verdin *et*
343 *al.*, 2005), and the oomycete *Pythium ultimum* (Furuno *et al.*, 2012). Intracellular PAH uptake thus
344 appears to occur in several fungal species regardless of PAH degradation efficiency.
345 Accumulation of lipophilic toxins in lipid bodies may be a defense mechanism against oxidative stress
346 in fungi. Indeed, Chang *et al.* (2015) found that the formation of large lipid bodies in *Candida albicans*
347 was associated with mycotoxin resistance, and that toxins were stored in lipid bodies. The authors
348 propose a protection mechanism against oxidative stress caused by the oxidation of aromatic rings,
349 involving quenching of reactive oxygen species by the triacyglycerols making up the bulk of storage
350 lipids. A similar strategy in *Talaromyces helicus* may serve as a protection against the adverse effects
351 of BaP and other lipophilic organic compounds.

352 Additionally, lipid bodies may be a site of intracellular degradation. Delsarte *et al.* (2018) proposed a
353 connection between BaP degradation and neutral lipid cycling in fungal cells, hypothesizing that BaP
354 stored in lipid bodies could be oxidized simultaneously as lipid beta-oxidation occurs in neighboring
355 peroxisomes.

356 **4.2. Preferential uptake at a close range**

357 Previous hypotheses on the uptake mechanisms of hydrophobic compounds suggest that growing
358 hyphal tips, which are metabolically active and host intense exchanges with the extracellular
359 environment, are preferential sites of uptake (Fayeulle *et al.*, 2014). In accordance with this
360 hypothesis, mycelium incubated with BaP frequently displays stained hyphal tips. Transport and
361 storage in older parts of the mycelium is suspected but not established. Indeed, stained lipid bodies
362 are visible in all parts of the mycelium, indicating that BaP is either incorporated in already formed
363 segments, or brought there from the tips through intrahyphal transport. Intrahyphal translocation of
364 PAH through vesicle streaming was observed in *P. ultimum* (Furuno *et al.*, 2012). However, although
365 cytoplasmic streaming was observed during our time-lapse experiments in bright field microscopy, no
366 evidence of lipid body movement was found in *T. helicus* with specific staining. Previous studies
367 suggest that lipid bodies in filamentous fungi originate from the endoplasmic reticulum, forming
368 small lipid bodies that later fuse into larger ones (Kamisaka *et al.*, 1999). Such early precursors of the
369 mature lipid bodies may be more mobile, but smaller than the camera resolution used for the present
370 experiments. Alternatively, BaP could be solubilized in membranes and be transported along with
371 vesicles to various organelles, in a similar way to neutral lipids and other lipophilic compounds
372 (Murphy *et al.*, 2009). Indeed, the IMPALA simulation results predict that the most stable position for
373 BaP in a lipid bilayer is within the hydrophobic core, which indicate a possible penetration into cell
374 membranes and subsequent lateral diffusion. The insertion of PAH into model lipid membranes was
375 also demonstrated experimentally (Castelli *et al.*, 2002). However it is very unlikely for BaP in the
376 molecular form to be present in water surrounding cells and to diffuse freely through the
377 extracellular aqueous medium at concentrations high enough to explain its effective biodegradation.

Thus for BaP to be absorbed into membranes, it would need to be already in close vicinity to the cell surface, either as crystals, or solubilized by surface-active molecules. Transport phenomena, other than passive diffusion, must therefore occur earlier than the cell membrane crossing in the incorporation process to bring the pollutant in contact with the cell surface.

Microscopic observations of *T. helicus* in spiked microfluidic chips indicate a preferential uptake of BaP at a close range and through contact with the cell wall. Indeed, when BaP is supplied as a fixed solid deposit in microfluidic chambers, fluorescent staining of the mycelium is the most intense after the deposit has been reached. This is consistent with observations in mycelium suspensions as well, since, when BaP crystals are dispersed in the liquid medium through continuous agitation, they can come into direct contact with hyphae and get trapped into the tightly knit mycelial network. As a result, the core of mycelial pellets frequently appears brightly stained as opposed to growing hyphae at the periphery. Moreover, early staining of some hyphae was observed before contact with BaP crystals in microfluidic chips. The staining was most often localized in some hyphal apices, sometimes highlighting the cell wall of older hyphae and lipid bodies in the cytoplasm. These results indicate that a long-range mobilization mechanism is at play, bringing BaP molecules to the fungal cells before hyphae could reach the solid crystals. The staining of cell walls observed on some occasions suggests that BaP adsorption to cell walls is a preliminary step to further internalization. Accumulation of BaP at the cell wall was previously shown in *F. solani* (Fayeulle *et al.*, 2014) when the formation of actin filaments is inhibited, preventing endocytosis and vesicle trafficking. In a context of non-inhibited metabolic activity, little to no staining of the cell wall is observed, indicating an equilibrium between cell wall adsorption rates and uptake rates.

4.3 Extracellular mobilization and transport

The access to the BaP deposits in crystal form relies either on hyphal growth up to the source, or on transport in water. Surface-active compounds may increase BaP partitioning into the water phase by accumulating at the surface of solid BaP particles and promote their fragmentation and dispersion in

the medium. This hypothesis seems in accordance with the observation that surfactants enable transfers of hydrophobic molecules between hydrophobic phases of an emulsion stabilized by solid particles (Drelich *et al.*, 2012). However, the possible role of fungal surfactants in BaP mobilization has not been elucidated so far.

The mechanisms involved in hydrophobic pollutant mobilization could be closely linked to the nutrition behaviour of filamentous fungi. Indeed, hydrophobic compounds in contaminated soils such as BaP are frequently associated with non-aqueous phase liquids and organic matter, which can readily be used by fungi as carbon sources. Some microbial surfactants are able to partially solubilize hydrophobic organic compounds (Ron and Rosenberg, 2002; Van Hamme *et al.*, 2006), including PAH (Garcia-Junco *et al.*, 2003; Sánchez-Vázquez *et al.*, 2018), thus enhancing their bioavailability. Sophorolipid biosurfactants excretion has also been linked to the degradation of anthracene sorbed to a solid matrix in several yeast species (Romero *et al.*, 2016). However in our study with *Talaromyces helicus*, no extracellular lipids were detected, excluding sophorolipids or other similar glycolipids from biosurfactants candidates. Interestingly, non-lipidic surface-active molecules have been described to play major roles in fungal interactions with hydrophobic substrates such as hydrophobins (Berger and Sallada, 2019) or exopolysaccharides (Mahapatra and Banerjee, 2013). This kind of molecules could be related to the surface tension decrease of culture filtrates observed in our study. Dissolved organic matter itself can serve as a mobilizing agent promoting hydrophobic organic compounds (HOC) dispersion in the water phase (Smith *et al.*, 2009, 2011). Biosurfactants could also promote the dispersal and transport of small solid particles or droplets of organic phases containing BaP. Additionally, fungal hyphae whose growth was oriented towards the source of nutrients following a gradient, may thus come into contact with associated pollutants. Facilitated transport of HOC in small amounts in the aqueous phase would thus be a preliminary step to direct contact and incorporation in greater amounts.

Although the main PAH biodegradation pathway in non-ligninolytic fungi is thought to be intracellular, fungi release a variety of extracellular enzymes involved in nutrition, including oxidoreductases such

as laccases, lignin peroxidases, manganese peroxidases, and tyrosinases which catalyze the production of oxidizing agents and free radicals leading to the non-specific oxidation of substrates (Tuomela and Hatakka, 2011). The fungal metabolism of aromatic compounds produces substituted derivatives that are more reactive and more soluble than the original pollutants like phenol, phthalate, hydroxyl-, carboxy- and dihydrodiol derivates that may in a second step be conjugated with sugar moieties (Boll *et al.*, 2015; Marco-Urrea *et al.*, 2015). Such metabolites display radically different behaviors compared to the parent PAHs, and tend to partition into the water phase at much higher rates, which could promote their absorption by micro-organisms and facilitate their transport through the cell membrane.

4.4 Fungal access to benzo[a]pyrene in compartmentalized environments

Taken together our results enable to propose a two-steps mechanism for the access to BaP by a non-ligninolytic fungus before its uptake and intracellular biodegradation in a compartmentalized microenvironment like soil. Firstly, a distant uptake was shown, which highlights an extracellular mobilization step possibly related to the surface-active agents detected in filtrates or to extracellular enzyme activities. This first step may increase the presence of BaP or associated hydrophobic compounds in the water phase and create gradients susceptible to drive growth to the pollutant source. Secondly uptake appears to be more efficient after the mycelium touches a BaP deposit , which could be explained by a better access to the pollutant through a direct chemical partitioning between BaP crystals and hydrophobic portions of the hyphae surfaces as suggested by the simulation. These mechanisms of mobilization and uptake could vary according to the physicochemical properties of the considered PAH and in particular its water solubility. Indeed the phenanthrene and BaP uptakes by *F. solani* showed different kinetics and were suggested to occur through different mechanisms (Fayeulle *et al.*, 2014). The better understanding of these active phenomena to reach hydrophobic pollutants is of relevance to enhance mycoremediation efficiency though biostimulation approaches, since low PAH bioavailability remains one of the major limitations

for the development of these techniques (Akhtar and Mannan, 2020). The elucidation of the mechanisms by which filamentous fungi influence PAH bioavailability in soils (Posada-Baquero *et al.*, 2019) and transport these molecules through the hyphal network (Harms *et al.*, 2011) are also important to understand how they can positively interact with other types of organisms within combined bioremediation strategies (Baranger *et al.*, 2021). Notably positive results in bioremediation of PAH impacted soils have been obtained through combination of mycoremediation and phytoremediation (Ma *et al.*, 2021).

5 Conclusion

A compartmentalized microchip was designed to observe the incorporation of benzo[a]pyrene by the fungus *Talaromyces helicus* in a controlled geometry. This is the first time to our knowledge that BaP fungal uptake is directly observed in a compartmentalized system and that a combination of extracellular surfactants and direct contact uptake is proposed to explain this phenomenon. Indeed the fungus is able to develop a mycelium in the confined chambers, and hyphae can grow in direct contact with BaP crystals. Observations through epifluorescence and confocal microscopy confirmed that the pollutant is incorporated into the cells of *T. helicus,* and co-staining experiments with BODIPY lipid dye show that lipid bodies are a preferential storage site in the cell. BaP uptake in *T. helicus* occurred even when hyphae were not directly touching the crystals, but to a lower extent than when hyphae were in direct contact with the crystals. Additionally, *T. helicus* produces extracellular surface-active compounds that were detected in culture filtrates. Thus, the use of a microfluidic device in our study brings first pieces of evidence for a two-steps mechanism involved in the access to BaP by a non-ligninolytic soil fungus before its uptake and intracellular biodegradation.

6 Fundings

C.B. benefited from a doctoral grant from the French Ministry of Research. The MycoFlu project has been supported by grants from the CNRS (EC2CO programme MICROBIEN) and Sorbonne Universités (programme Emergence, SU-16-R-EMR-28).

7 Aknowledgements

The authors would like to thank Sandrine Lelong-Caristan and the society Chromacim for their support in HPTLC analyses. The authors are also grateful to Xue Sun, Alicia Alejandra Mier Gonzalez, Marie Valmori, Roxane Valentin and Théo Guillerm for their help with the preliminary experiments.

8 Bibliography

1 Akhtar, N., & Mannan, M. A., 2020. Mycoremediation : Expunging environmental pollutants. Biotechnol. Rep. 26, e00452. https://doi.org/10.1016/j.btre.2020.e00452

2 Al-Hawash, A.B., Zhang, X., Ma, F., 2019. Removal and biodegradation of different petroleum hydrocarbons using the filamentous fungus *Aspergillus sp.* RFC-1. MicrobiologyOpen 8, e00619. https://doi.org/10.1002/mbo3.619

3 Aleklett, K., Kiers, E. T., Ohlsson, P., Shimizu, T. S., Caldas, V. E., Hammer, E. C., 2018. Build your own soil: exploring microfluidics to create microbial habitat structures. The ISME Journal 12, 312-319. https://doi.org/10.1038/ismej.2017.184

4 Alnahhas, R.N., Winkle, J.J., Hirning, A.J., Karamched, B., Ott, W., Josić, K., Bennett, M.R., 2019. Spatiotemporal Dynamics of Synthetic Microbial Consortia in Microfluidic Devices. ACS Synth. Biol. 8, 2051–2058. https://doi.org/10.1021/acssynbio.9b00146

5 Arutchelvi, J.I., Bhaduri, S., Uppara, P.V., Doble, M., 2008. Mannosylerythritol lipids: a review. J. Ind. Microbiol. Biotechnol. 35, 1559–1570. https://doi.org/10.1007/s10295-008-0460-4

6 Baranger, C., Fayeulle, A., Le Goff, A., 2020. Microfluidic monitoring of the growth of individual hyphae in confined environments. R. Soc. open sci. 7, 191535. https://doi.org/10.1098/rsos.191535

7 Baranger, C., Pezron, I., Le Goff, A., Fayeulle, A, 2021. Fungal influence on hydrophobic organic pollutants dynamics within the soil matrices, In: Rhizomicrobe Dynamics in Bioremediation, V. Kumar Editor, CRC Press, ISBN 9780367419660, 2021, Chapter 1, 1-27. https://doi.org/10.1201/9780367821593-1

8 Berger, B. W., Sallada, N. D., 2019. Hydrophobins : Multifunctional biosurfactants for interface engineering. J. Biol. Eng. 13, 10. https://doi.org/10.1186/s13036-018-0136-1

9 Boll, E.S., Johnsen, A.R., Christensen, J.H., 2015. Polar metabolites of polycyclic aromatic compounds from fungi are potential soil and groundwater contaminants. Chemosphere 119, 250–257. https://doi.org/10.1016/j.chemosphere.2014.06.033

10 Castelli, F., Librando, V., Sarpietro, M.G., 2002. Calorimetric Approach of the Interaction and Absorption of Polycyclic Aromatic Hydrocarbons with Model Membranes. Environ. Sci. Technol. 36, 2717–2723. https://doi.org/10.1021/es010260w

11 Cerniglia, C.E., Sutherland, J.B., 2010. Degradation of polycyclic aromatic hydrocarbons by fungi, in: Timmis, K.N. (Ed.), Handbook of Hydrocarbon and Lipid Microbiology. Springer Berlin Heidelberg, Berlin, Heidelberg, pp. 2079–2110.

12 Chang, W., Zhang, M., Zheng, S., Li, Y., Li, X., Li, W., Li, G., Lin, Z., Xie, Z., Zhao, Z., Lou, H., 2015. Trapping toxins within lipid droplets is a resistance mechanism in fungi. Sci. Rep. 5, 1–11. https://doi.org/10.1038/srep15133

13 Črešnar, B., Petrič, Š., 2011. Cytochrome P450 enzymes in the fungal kingdom. BBA - Proteins Proteom. 1814, 29–35. https://doi.org/10.1016/j.bbapap.2010.06.020

14 Delsarte, I., Rafin, C., Mrad, F., Veignie, E., 2018. Lipid metabolism and benzo[*a*]pyrene degradation by *Fusarium solani*: an unexplored potential. Environ. Sci. Pollut. Res. 25, 12177–12182. https://doi.org/10.1007/s11356-017-1164-y

15 Drelich, A., Grossiord, J.-L., Gomez, F., Clausse, D., Pezron, I., 2012. Mixed O/W emulsions stabilized by solid particles : A model system for controlled mass transfer triggered by surfactant addition. J. Colloid Interface Sci. 386, 218–227. https://doi.org/10.1016/j.jcis.2012.07.072

16 Dreyer, B., Morte, A., Pérez-Gilabert, M., Honrubia, M., 2006. Autofluorescence detection of arbuscular mycorrhizal fungal structures in palm roots: an underestimated experimental method. Mycol. Res. 110, 887–897. https://doi.org/10.1016/j.mycres.2006.05.011

17 Ducarme, Ph., Rahman, M., Brasseur, R., 1998. IMPALA: A simple restraint field to simulate the biological membrane in molecular structure studies. Proteins 30, 357–371.

18 Fayeulle, A., 2013. Etude des mécanismes intervenant dans la biodégradation des Hydrocarbures Aromatiques Polycycliques par les champignons saprotrophes telluriques en vue d'applications en bioremédiation fongique de sols pollués. Université du Littoral Côte d'Opale, Dunkerque.

19 Fayeulle, A., Veignie, E., Schroll, R., Munch, J.C., Rafin, C., 2019. PAH biodegradation by telluric saprotrophic fungi isolated from aged PAH-contaminated soils in mineral medium and historically contaminated soil microcosms. J. Soils Sediments 19, 3056–3067. https://doi.org/10.1007/s11368-019-02312-8

20 Fayeulle, A., Veignie, E., Slomianny, C., Dewailly, E., Munch, J.-C., Rafin, C., 2014. Energy-dependent uptake of benzo[*a*]pyrene and its cytoskeleton-dependent intracellular transport by the telluric fungus *Fusarium solani*. Environ. Sci. Pollut. Res. 21, 3515–3523. https://doi.org/10.1007/s11356-013-2324-3

21 Furuno, S., Foss, S., Wild, E., Jones, K.C., Semple, K.T., Harms, H., Wick, L.Y., 2012. Mycelia promote active transport and spatial dispersion of polycyclic aromatic hydrocarbons. Environ. Sci. Technol. 46, 5463–5470. https://doi.org/10.1021/es300810b

22 Garay, L.A., Sitepu, I.R., Cajka, T., Xu, J., Teh, H.E., German, J.B., Pan, Z., Dungan, S.R., Block, D.E., Boundy-Mills, K.L., 2018. Extracellular fungal polyol lipids: A new class of potential high value lipids. Biotechnol. Adv. 36, 397–414.

23 Garcia-Junco, M., Gomez-Lahoz, C., Niqui-Arroyo, J.-L., Ortega-Calvo, J.-J., 2003. Biosurfactant- and biodegradation-enhanced partitioning of polycyclic aromatic hydrocarbons from nonaqueous-phase liquids. Environ. Sci. Technol. 37, 2988–2996. https://doi.org/10.1021/es020197q

24 Grossmann, G., Guo, W.-J., Ehrhardt, D.W., Frommer, W.B., Sit, R.V., Quake, S.R., Meier, M., 2011. The RootChip: An Integrated Microfluidic Chip for Plant Science. The Plant Cell 23, 4234–4240. https://doi.org/10.1105/tpc.111.092577

25 Harms, H., Schlosser, D., Wick, L. Y., 2011. Untapped potential : Exploiting fungi in bioremediation of hazardous chemicals. Nat. Rev. Microbiol. 9, 177−192. https://doi.org/10.1038/nrmicro2519

26 Held, M., Lee, A.P., Edwards, C., Nicolau, D.V., 2010. Microfluidics structures for probing the dynamic behaviour of filamentous fungi. Microelectron. Eng. 87, 786–789. https://doi.org/10.1016/j.mee.2009.11.096

27 Huang, L.H., Schmitt, J.A., 1975. Ohio ascomycete notes II. *Talaromyces* from soils of southern Ohio. Ohio J. Sci. 75, 75–81.

28 Jabaji-Hare, S.H., Perumalla, C.J., Kendrick, W.B., 1984. Autofluorescence of vesicles, arbuscules, and intercellular hyphae of a vesicular–arbuscular fungus in leek (*Allium porrum*) roots. Can. J. Botany 62, 2665–2669.

29 Jennings, A.A., 2012. Worldwide regulatory guidance values for surface soil exposure to carcinogenic or mutagenic polycyclic aromatic hydrocarbons. J. Environ. Manage. 110, 82–102. https://doi.org/10.1016/j.jenvman.2012.05.015

30 Kamisaka, Y., Noda, N., Sakai, T., Kawasaki, K., 1999. Lipid bodies and lipid body formation in an oleaginous fungus, *Mortierella ramanniana* var. *angulispora*. BBA - Mol. Cell Biol. L. 1438, 185–198. https://doi.org/10.1016/S1388-1981(99)00050-5

31 Käppeli, O., Walther, P., Mueller, M., Fiechter, A., 1984. Structure of the cell surface of the yeast *Candida tropicalis* and its relation to hydrocarbon transport. Arch. Microbiol. 138, 279–282. https://doi.org/10.1007/BF00410890

32 Kuppusamy, S., Thavamani, P., Venkateswarlu, K., Lee, Y.B., Naidu, R., Megharaj, M., 2016. Remediation approaches for polycyclic aromatic hydrocarbons (PAHs) contaminated soils: Technological constraints, emerging trends and future directions. Chemosphere 168, 944–968. https://doi.org/10.1016/j.chemosphere.2016.10.115

33 Leriche-Grandchamp, M., Flourat, A., Shen, H., Picard, F., Giordana, H., Allais, F., Fayeulle, A., 2020. Inhibition of phenolics uptake by ligninolytic fungal cells and its potential as a tool for the production of lignin-derived aromatic building blocks. J. Fungi 6, 362. https://doi.org/10.3390/jof6040362

34 Lindley, N.D., Heydeman, M.T., 1986. Mechanism of dodecane uptake by whole cells of *Cladosporium resinae*. Microbiology 132, 751–756. https://doi.org/10.1099/00221287-132-3-751

35 Ma, X., Li, X., Liu, J., Cheng, Y., Zou, J., Zhai, F., Sun, Z., Han, L., 2021. Soil microbial community succession and interactions during combined plant/white-rot fungus remediation of polycyclic aromatic hydrocarbons. Sci. Total Environ. 752, 142224. https://doi.org/10.1016/j.scitotenv.2020.142224

36 Mahapatra, S., Banerjee, D., 2013. Fungal exopolysaccharide : Production, composition and applications. Microbiol. Insights 6, 1−16. https://doi.org/10.4137/MBI.S10957

37 Marco-Urrea, E., García-Romera, I., Aranda, E., 2015. Potential of non-ligninolytic fungi in bioremediation of chlorinated and polycyclic aromatic hydrocarbons. New Biotechnol., European Congress of Biotechnology - ECB 16 32, 620–628. https://doi.org/10.1016/j.nbt.2015.01.005

38 Moore, D., Robson, G.D., Trinci, A.P.J., 2015. 21st Century Guide to Fungi. Cambridge University Press.

39 Murphy, S., Martin, S., Parton, R.G., 2009. Lipid droplet-organelle interactions; sharing the fats. BBA - Mol. Cell Biol. L. 1791, 441–447. https://doi.org/10.1016/j.bbalip.2008.07.004

40 Olagoke, O.A., 2014. Amylase activities of some thermophilic fungi isolated from municipal solid wastes and palm-kernel stack. Am. J. Microbiol. Biotechnol. 1, 64–70.

41 Ortega-Calvo, J.J., Tejeda-Agredano, M.C., Jimenez-Sanchez, C., Congiu, E., Sungthong, R., Niqui-Arroyo, J.L., Cantos, M., 2013. Is it possible to increase bioavailability but not environmental risk of PAHs in bioremediation? J. Hazard. Mater. 261, 733–745. https://doi.org/10.1016/j.jhazmat.2013.03.042

42 Panagos, P., Van Liedekerke, M., Yigini, Y., Montanarella, L., 2013. Contaminated sites in Europe: Review of the current situation based on data collected through a european network. J. Environ. Pub. Health 2013, 1–11. https://doi.org/10.1155/2013/158764

43 Posada-Baquero, R., Martín, M. L., Ortega-Calvo, J.-J., 2019. Implementing standardized desorption extraction into bioavailability-oriented bioremediation of PAH-polluted soils. Sci. Total Environ. 696, 134011. https://doi.org/10.1016/j.scitotenv.2019.134011

44 Puchkov, E.O., Zähringer, U., Lindner, B., Kulakovskaya, T.V., Seydel, U., Wiese, A., 2002. The mycocidal, membrane-active complex of *Cryptococcus humicola* is a new type of cellobiose lipid with detergent features. BBA - Biomembranes 1558, 161–170. https://doi.org/10.1016/S0005-2736(01)00428-X

45 Rayu, S., Karpouzas, D.G., Singh, B.K., 2012. Emerging technologies in bioremediation: constraints and opportunities. Biodegradation 23, 917–926. https://doi.org/10.1007/s10532-012-9576-3

46 Romero, M.C., Chiaravalli, J.C., Reinoso, E.H., 2016. Sorbed anthracene degradation by sophorolipid producing yeasts. Int. J. Biotech Well. Indus. 5, 25-31–31.

47 Romero, M.C., Hammer, E., Hanschke, R., Arambarri, A.M., Schauer, F., 2005. Biotransformation of biphenyl by the filamentous fungus *Talaromyces helicus*. World J. Microb. Biot. 21, 101–106. https://doi.org/10.1007/s11274-004-2779-y

48 Romero, M.C., Urrutia, M.I., Reinoso, E.H., Moreno Kiernan, A., 2009. Wild soil fungi able to degrade the herbicide isoproturon. Rev. Mex. Micol. 29, 1–7.

49 Romero, M.C., Urrutia, M.I., Reinoso, H.E., Kiernan, M.M., 2010. Benzo[*a*]pyrene degradation by soil filamentous fungi. J. Yeast Fungal Res. 1, 025–029.

50 Ron, E.Z., Rosenberg, E., 2002. Biosurfactants and oil bioremediation. Curr. Opin. Biotechnol. 13, 249–252. https://doi.org/10.1016/S0958-1669(02)00316-6

51 Sánchez-Vázquez, V., Shirai, K., González, I., Gutiérrez-Rojas, M., 2018. Polycyclic aromatic hydrocarbon-emulsifier protein produced by *Aspergillus brasiliensis (niger)* in an airlift bioreactor following an electrochemical pretreatment. Biores. Technol. 256, 408–413. https://doi.org/10.1016/j.biortech.2018.02.043

52 Scervino, J.M., Mesa, M.P., Della Mónica, I., Recchi, M., Sarmiento Moreno, N., Godeas, A., 2010. Soil fungal isolates produce different organic acid patterns involved in

phosphate salts solubilization. Biol. Fertil. Soil 46, 755–763. https://doi.org/10.1007/s00374-010-0482-8

53 Smith, K.E.C., Thullner, M., Wick, L.Y., Harms, H., 2011. Dissolved organic carbon enhances the mass transfer of hydrophobic organic compounds from nonaqueous phase liquids (NAPLs) into the aqueous phase. Environ. Sci. Technol. 45, 8741–8747. https://doi.org/10.1021/es202983k

54 Smith, K.E.C., Thullner, M., Wick, L.Y., Harms, H., 2009. Sorption to humic acids enhances polycyclic aromatic hydrocarbon biodegradation. Environ. Sci. Technol. 43, 7205–7211. https://doi.org/10.1021/es803661s

55 Squires, T.M., Quake, S.R., 2005. Microfluidics: Fluid physics at the nanoliter scale. Rev. Mod. Phys. 77, 977–1026. https://doi.org/10.1103/RevModPhys.77.977

56 Tuomela, M., Hatakka, A., 2011. Oxidative fungal enzymes for bioremediation, in: Industrial and Toxic Wastes. Elsevier, pp. 183–196.

57 Van Hamme, J.D., Singh, A., Ward, O.P., 2006. Physiological aspects: Part 1 in a series of papers devoted to surfactants in microbiology and biotechnology. Biotechnology Advances 24, 604–620. https://doi.org/10.1016/j.biotechadv.2006.08.001

58 Verdin, A., Lounès-Hadj Sahraoui, A., Newsam, R., Robinson, G., Durand, R., 2005. Polycyclic aromatic hydrocarbons storage by *Fusarium solani* in intracellular lipid vesicles. Environ. Pollut. 133, 283–291. https://doi.org/10.1016/j.envpol.2004.05.040

59 Vidali, M., 2001. Bioremediation. an overview. Pure Appl. Chem. 73, 1163–1172. https://doi.org/10.1351/pac200173071163

60 Wilpiszeski, R.L., Aufrecht, J.A., Retterer, S.T., Sullivan, M.B., Graham, D.E., Pierce, E.M., Zablocki, O.D., Palumbo, A.V., Elias, D.A., 2019. Soil aggregate microbial communities:

Towards understanding microbiome interactions at biologically relevant scales. Appl. Environ. Microbiol. 85, e00324-19. https://doi.org/10.1128/AEM.00324-19

61 Wu, H., Wu, L., Wang, J., Zhu, Q., Lin, S., Xu, J., Zheng, C., Chen, J., Qin, X., Fang, C., Zhang, Z., Azeem, S., Lin, W., 2016. Mixed phenolic acids mediated proliferation of pathogens *Talaromyces helicus* and *Kosakonia sacchari* in continuously monocultured *Radix pseudostellariae* rhizosphere soil. Front. Microbiol. 7, 335. https://doi.org/10.3389/fmicb.2016.00335

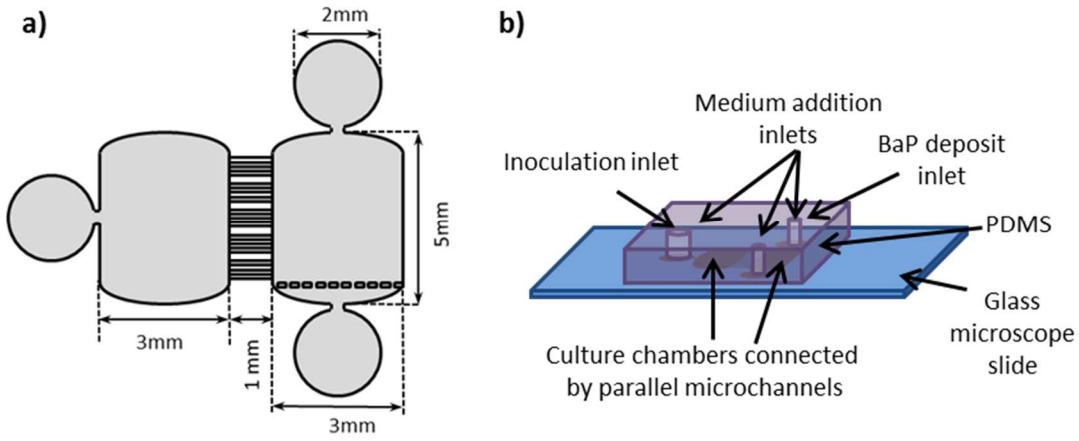

Fig. 1: Diagram representing the microfluidic device used for fungal cultivation in presence of BaP. a. channel geometry. b. experimental set-up.

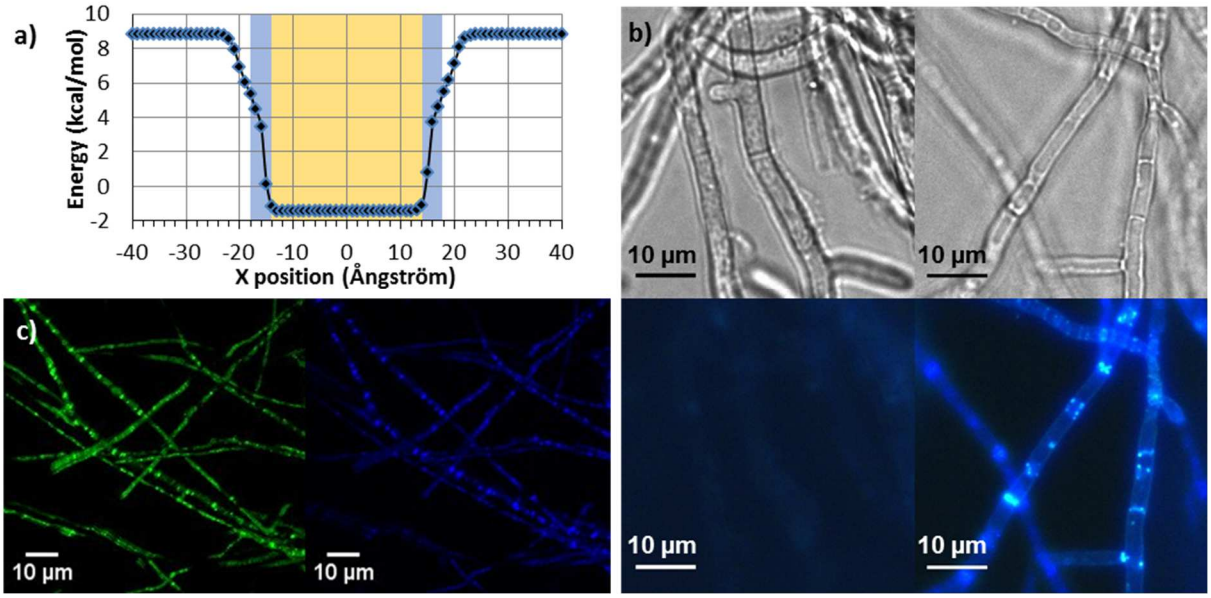

Fig. 2 : a - Simulation of BaP penetration across a model lipid bilayer using the IMPALA method. X-axis: position of the mass center of BaP relatively to the center of the lipid bilayer; Y-axis: interaction energy calculated as described in Methods. The different regions of the membrane are highlighted in yellow (core hydrocarbon chains) and blue (polar heads). b - Mycelium of *T. helicus* after 24 h of incubation with or without BaP, observed in bright field (top row) and epifluorescence using the DAPI excitation filter (bottom row). left: control mycelium without BaP, showing a faint cell wall autofluorescence; right: mycelium incubated with BaP, displaying small stained vesicles localized at the periphery of hyphal segments. c - Mycelium of *T. helicus* incubated with BaP and stained with BODIPY, observed in confocal microscopy at 40 x magnification (maximum intensity projection of a 41 images stack with a 0.38 µm increment, false colors). Left: FITC filter (green); right: DAPI filter (blue). Both color channels show fluorescent staining colocalized in intracellular vesicles.

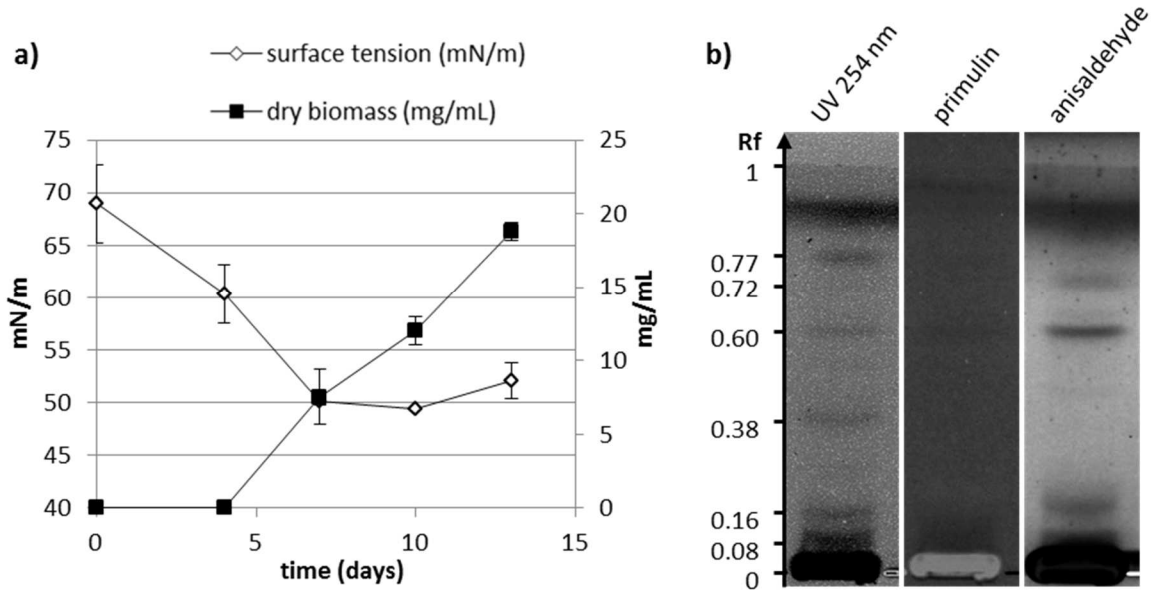

Fig. 3: Detection of surface-active compounds in culture supernatants of *T. helicus* grown in plain mineral medium. a - surface tension of the cell-free supernatant and dry fungal biomass over time. b – HPLTC analysis of a 13-day supernatant sample. From left to right: observation under UV light at 254 nm to reveal organic compounds, after primulin staining to detect lipids at 366 nm, and after anisaldehyde staining to detect carbohydrates under white light.

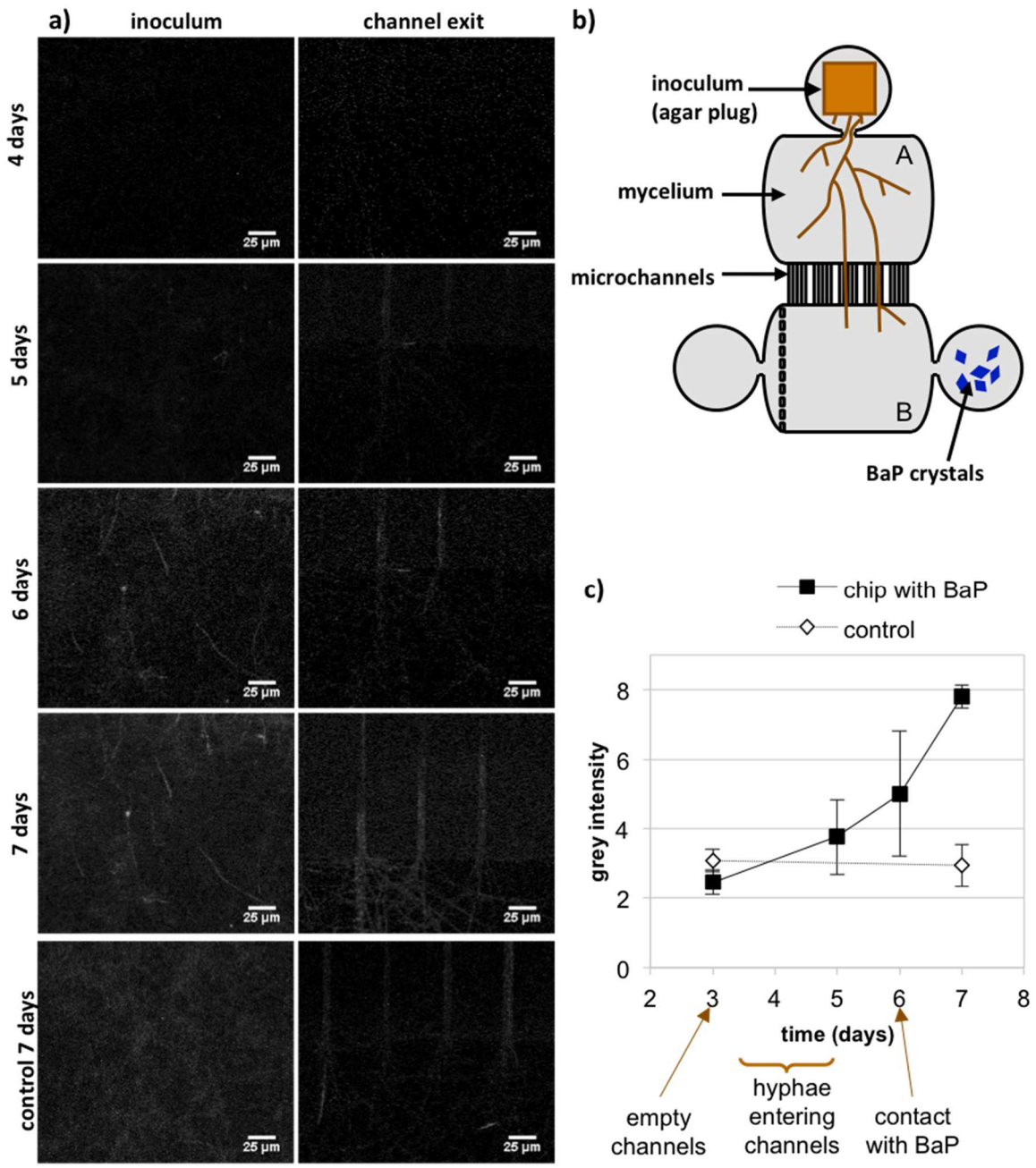

Fig 4 : a. Mycelium of *T. helicus* growing in a microfluidic chip spiked with BaP, observed in LSCM at 20x magnification (maximal intensity projection of image stacks with a 1 µm increment). Left column: Images taken in chamber A (inoculum). Right column: Images taking at the opening of microchannels on the side of chamber B (BaP deposit). b. Diagram representing the microfluidic device used for fungal cultivation in presence of BaP. c. Variation of fluorescence intensity over time, as represented by the average grey intensity measured in three microchannels in the same microchip over a 10x100 µm area (error bars represent the standard deviation of each triplicate; arrows indicate the grey intensity of empty channels, the hyphae entrance in channels and the time after which the direct contact between mycelium and BaP occurred in the considered chip).

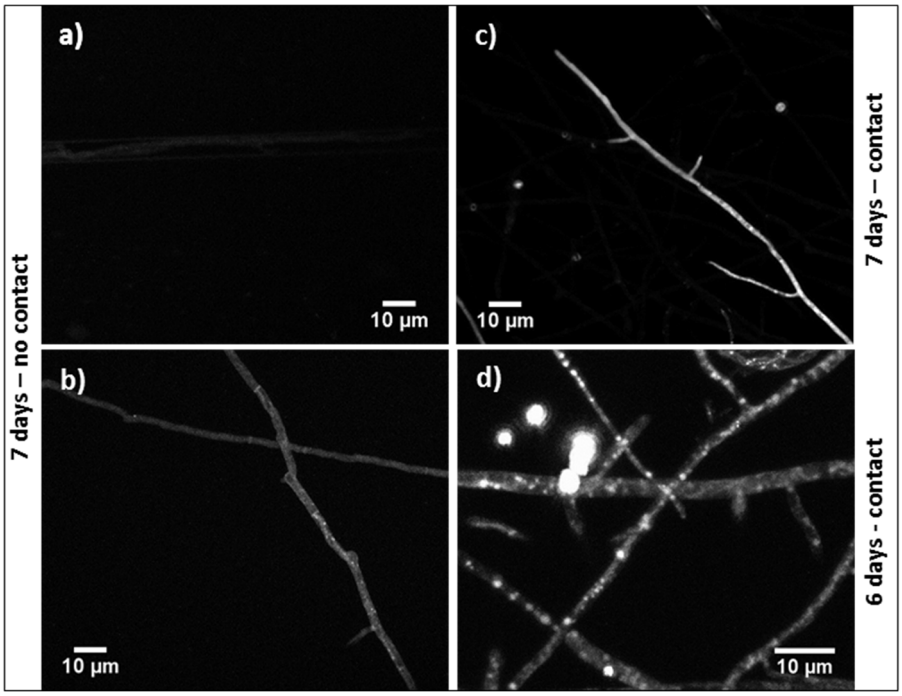

Fig. 5: Mycelium of *T. helicus* growing in microfluidic chips spiked with BaP, observed in LSCM at 40x magnification after 6 to 7 days of incubation. (maximum intensity projection of image stacks with a 1 µm increment). a. Detail of hyphae growing in a microchannel before the mycelium reached the BaP deposit – b. Detail of hyphae growing in chamber B. after the mycelium grew through the channels but not yet reached the BaP deposit. c. Stained hyphal tips in chamber B, close to the BaP deposit. d. Hyphae displaying stained intracellular lipid bodies in chamber B, in direct contact with BaP crystals.

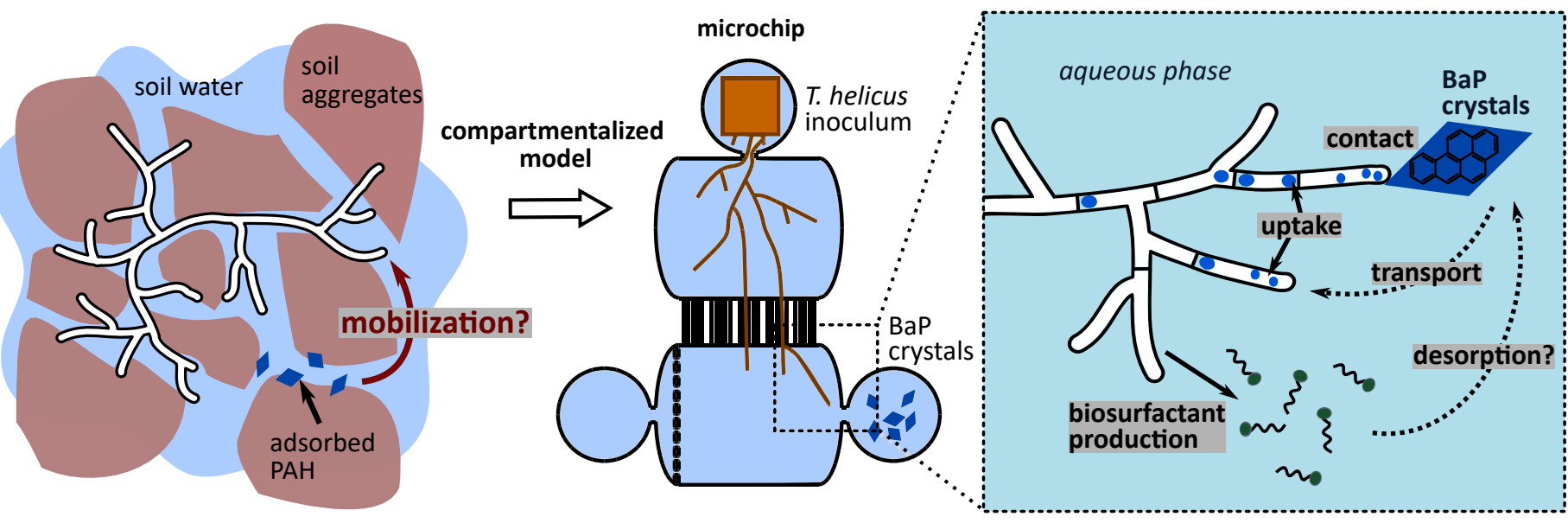
soil water
soil aggregates
mobilization?
adsorbed PAH
compartmentalized model
microchip
T. helicus inoculum
BaP crystals
aqueous phase
BaP crystals
contact
uptake
transport
desorption?
biosurfactant production